SPECTRAL IRRADIANCE CALIBRATION IN THE INFRARED. VII. NEW COMPOSITE SPECTRA, COMPARISON WITH MODEL ATMOSPHERES, AND FAR-INFRARED EXTRAPOLATIONS

NASA-CR-203117

MARTIN COHEN

Radio Astronomy Laboratory, 601 Campbell Hall, University of California, Berkeley, California 94720, and Jamieson Science and Engineering, Inc., Suite 204, 5321 Scotts Valley Drive, Scotts Valley, California 95066
Electronic mail: cohen@bkyast.berkeley.edu

FRED C. WITTEBORN

Space Science Division, Mailstop 245-6, NASA-Ames Research Center, Moffett Field, California 94035
Electronic mail: witteborn@ssa1.arc.nasa.gov

DUANE F. CARBON

NAS Systems Division, Mailstop 258-5, NASA-Ames Research Center, Moffett Field, California 94035
Electronic mail: dcarbon@nas.nasa.gov

JOHN K. DAVIES

Joint Astronomy Centre Hawaii, 660 N. Aohoku Place, University Park, Hilo, Hawaii 96720
Electronic mail: jkd@jach.hawaii.edu

DIANE H. WOODEN

Space Science Division, Mailstop 245-6, NASA-Ames Research Center, Moffett Field, California 94035
Electronic mail: wooden@ssa1.arc.nasa.gov

JESSE D. BREGMAN

Space Science Division, Mailstop 245-6, NASA-Ames Research Center, Moffett Field, California 94035
Electronic mail: bregman@ssa1.arc.nasa.gov

ABSTRACT

We present five new absolutely calibrated continuous stellar spectra constructed as far as possible from spectral fragments observed from the ground, the *Kuiper Airborne Observatory (KAO)*, and the *IRAS* Low Resolution Spectrometer. These stars—α Boo, γ Dra, α Cet, γ Cru, and μ UMa—augment our six, published, absolutely calibrated spectra of K and early-M giants. All spectra have a common calibration pedigree. A revised composite for α Boo has been constructed from higher quality spectral fragments than our previously published one. The spectrum of γ Dra was created in direct response to the needs of instruments aboard the *Infrared Space Observatory (ISO)*; this star's location near the north ecliptic pole renders it highly visible throughout the mission. We compare all our low-resolution composite spectra with Kurucz model atmospheres and find good agreement in shape, with the obvious exception of the SiO fundamental, still lacking in current grids of model atmospheres. The CO fundamental seems slightly too deep in these models, but this could reflect our use of generic models with solar metal abundances rather than models specific to the metallicities of the individual stars. Angular diameters derived from these spectra and models are in excellent agreement with the best observed diameters. The ratio of our adopted Sirius and Vega models is vindicated by spectral observations. We compare *IRAS* fluxes predicted from our cool stellar spectra with those observed and conclude that, at 12 and 25 μm, flux densities measured by *IRAS* should be revised downwards by about 4.1% and 5.7%, respectively, for consistency with our absolute calibration. We have provided extrapolated continuum versions of these spectra to 300 μm, in direct support of *ISO* (PHT and LWS instruments). These spectra are consistent with *IRAS* flux densities at 60 and 100 μm. © 1996 American Astronomical Society.

1. INTRODUCTION

The previous papers of this series have presented a consistent effort to provide absolutely calibrated broadband and narrowband infrared photometry and spectra based upon a carefully selected, infrared-customized pair of stellar models for Vega and Sirius, created by Kurucz, and absolutely calibrated by Cohen *et al.* (1992a, hereafter referred to as Paper I). These hot stellar models have been employed as reference spectra to provide continuous (i.e., uninterrupted in wave-

length), observed, absolutely calibrated spectra ("composites") of cool stars by the methods detailed by Cohen *et al.* (1992, hereafter referred to as Paper II) and Cohen *et al.* (1995, hereafter referred to as Paper IV). This approach has yielded six infrared-bright secondary stellar standards with calibration pedigrees directly traceable to our primary radiometric standard, namely, α CMa. Molecular bands of CO and SiO dominate these observed infrared spectra of cool giants and supergiants (Cohen *et al.* 1992b, hereafter referred to as Paper III).

In the present paper we update the spectrum of α Boo to take account of newer and higher quality spectral fragments, and we augment the six composites by spectra of four additional stars assembled by the identical procedures to those described in Papers II and IV (Sec. 2). Note that two of these new composites do not start at 1.2 μm because there has never been any further development of the unique Strecker *et al.* (1979, hereafter referred to as SEW) archive of airborne 1.2–5.5 μm spectra. The composite of μ UMa starts at about 3.1 μm, and that for γ Cru at about 3.9 μm. However, these can still provide valuable calibrators (cf. Cohen *et al.* 1996a, hereafter referred to as Paper VI which offers 3.0–29 μm coverage).

In a future paper (Cohen *et al.* 1996b, hereafter referred to as Paper VIII), we will describe how we have converted this limited set of stars with abundant spectral observations into a network of nearly 300 calibrators across the sky by using the "template assumption," namely, that the dereddened infrared spectrum of any observed K-M giant accurately represents the intrinsic spectrum of any other giant with the identical spectral type as the composite, and so serves as a "template." Given our intended dependence upon these few observed continuous spectra (now covering the range K0 −M3.4 III), it is appropriate to make direct comparisons with a grid of model atmospheres. We, therefore, compare Kurucz (1991, 1993) models for our stars with composite spectra, and ratio these calibrated spectra to the models (Sec. 3).

We have several objectives in these comparisons: to test the goodness of fit (shape) of theory and observations (these cool stellar models are totally independent of the data and procedures used to assemble the composites); if well matched in shape, to determine angular diameters from the normalization of models that match the composites; to compare these empirical angular diameters with those observed by Michelson (intensity) interferometry or lunar occultation; and to attempt the extrapolation of these observed spectra to the far-infrared, using *IRAS* measurements to attempt to validate these extrapolations. Despite the conspicuous omission of the SiO fundamental (whose presence locally dominates these spectra between about 7.5 and 12 μm), we find that the Kurucz models are capable of replicating these complete spectral shapes to within a few percent. Our derived angular diameters are in good accord with the best, observationally determined, diameters for these stars (Sec. 4).

We have sought direct observational evidence on the ratio of our adopted spectra of Sirius and Vega, both photometrically and through 10 μm spectroscopy, and find support for this ratio (Sec. 5).

TABLE 1. New composite spectra described in this paper.*

Star	Spectral type	Date of assembly
α Boo	K1 III	December 21, 1995
γ Dra	K5 III	December 22, 1995
α Cet	M1.5 III	March 26, 1996
γ Cru	M3.4 III	March 13, 1996
μ UMa	M0 III	April 2,1996

*Table 1 can be found in the AAS CD-ROM Series, Vol. 7, 1996.

In Sec. 6, we return to the issue of the mid-infrared behavior of real giants, as opposed to model atmospheres, and present empirical evidence in favor of the locally Rayleigh–Jeans character of K and M giants beyond 10 μm.

Finally, we again probe the absolute calibration of *IRAS* (cf. Paper I) by synthesizing *IRAS* flux densities for all our composites in the 12 and 25 μm bands (Sec. 7) and, from theoretical continuum extrapolations of their spectra using a grid computed by one of us (D.F.C) (Sec. 8), in the 60 and 100 μm bands (Sec. 9). We find good agreement between these extrapolated models and observed *IRAS* long-wavelength flux densities, encouraging us to provide stellar calibration spectra in support of *ISO*'s absolute calibration.

2. NEW COMPOSITE SPECTRA

Our methodology for creating a complete and continuous composite spectrum from 1.2 to 35 μm follows that described in Papers II and IV. Except for that of γ Cru, these new complete spectra were made possible through a fruitful collaboration with the UKIRT Service Observing program (cf. Cohen & Davies 1995, hereafter referred to as Paper V) that has provided high quality 10 and 20 μm spectral fragments. Table 1 summarizes the new composites. Full details of the process of assembly for each composite appear in the AAS CD-ROM Series, Vol. 7, 1996 associated with this paper, including the independent photometry used to support the normalization of spectral fragments. To illustrate the calibration pedigree that accompanies each new composite spectrum, we present only one table here, corresponding to α Boo. Figure 1 presents the spectra themselves in the form of $\log \lambda^4 F_\lambda$ vs $\log \lambda$ plots. We show the three composites with fullest wavelength coverage before those with more restricted ranges.

All the new spectral fragments incorporated into this paper were secured with two or more of the following instruments: the NASA-Ames "SIRAS" (Short Wavelength Infrared Array Spectrometer: Wooden 1989), "FOGS" (Faint Object Grating Spectrometer: Witteborn & Bregman 1984), or "HIFOGS" (High-efficiency Infrared Faint Object Grating Spectrometer: Witteborn *et al.* 1995) on the *KAO* or with the NASA 1.5 m Mt Lemmon telescope; the CGS3 spectrometer on the 3.8 m UKIRT; or the *IRAS* Low Resolution Spectrometer-(hereafter referred to as LRS). The Ames spectrometers are doubly sampled by using two different grating settings spaced an integral number plus one half detectors apart to achieve Nyquist sampling and to provide coverage of occasional dead detectors. CGS3 is always either doubly
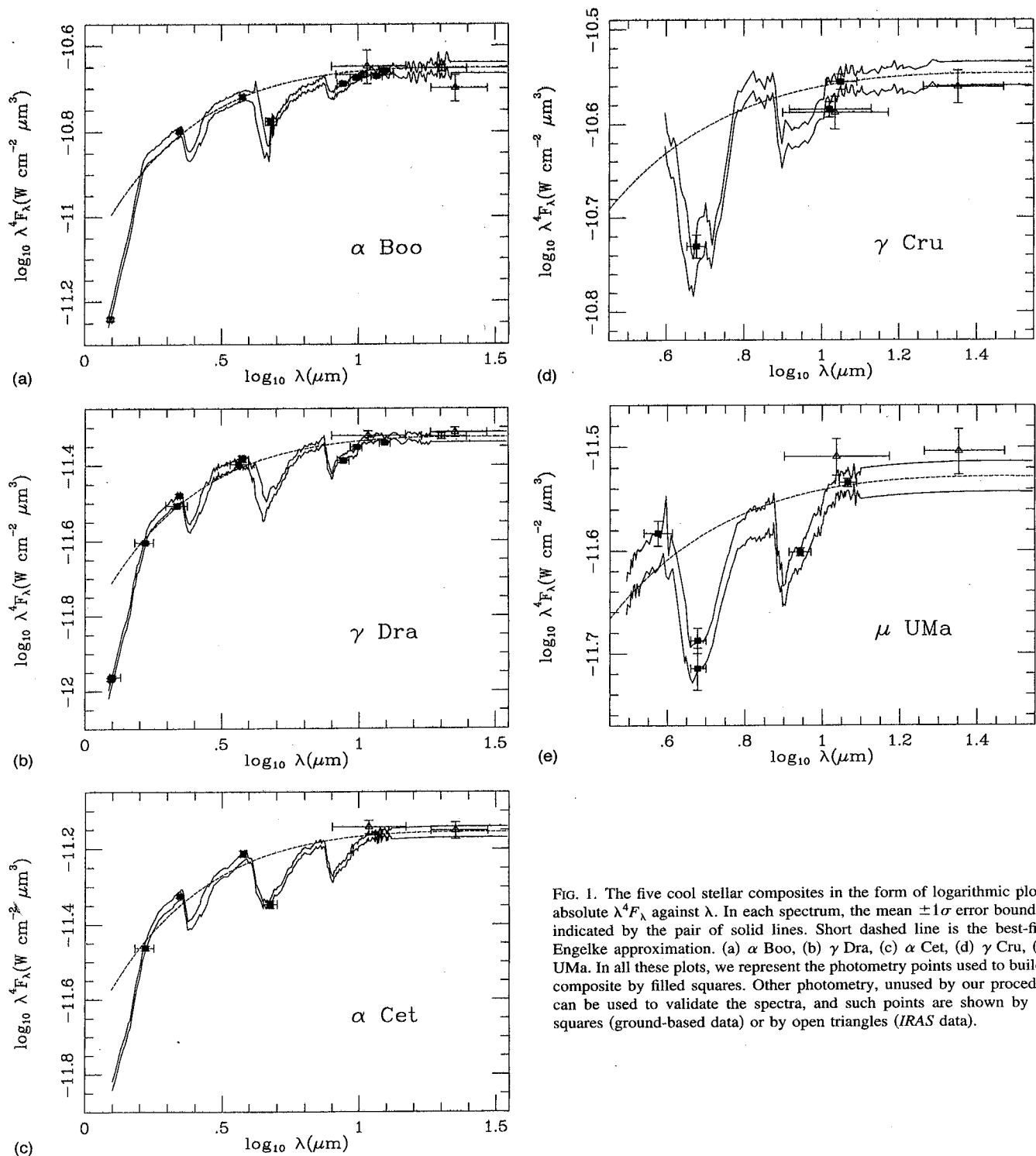
FIG. 1. The five cool stellar composites in the form of logarithmic plots of absolute $\lambda^4 F_\lambda$ against λ. In each spectrum, the mean $\pm 1\sigma$ error bounds are indicated by the pair of solid lines. Short dashed line is the best-fitting Engelke approximation. (a) α Boo, (b) γ Dra, (c) α Cet, (d) γ Cru, (e) μ UMa. In all these plots, we represent the photometry points used to build the composite by filled squares. Other photometry, unused by our procedures, can be used to validate the spectra, and such points are shown by open squares (ground-based data) or by open triangles (*IRAS* data).

or triply sampled, likewise to achieve the full theoretical resolution. For the CGS3 fragments (cf. Paper V) we have continued to emphasize close matching of airmasses between the cool target stars and the reference object (preferably Sirius, or one of our already established cool composites). From the *KAO* we could not always exert such control over stellar airmasses at the time of observation due to the relative brevity and constraints of the actual observing time at alti-

tude. Therefore, we remove the residual effects of the terrestrial atmosphere (particularly important from 5 to 8 μm) post facto from the spectra, through use of precomputed standard atmospheric transmission curves relevant to different amounts of precipitable water vapor (currently between 6 and 12 μm). Actual water vapor was measured on each flight with a radiometer. These transmissions were calculated using Lord's (1992) "ATRAN" software tool. Any corrections to

TABLE 2. Engelke functions used in, or relevant to, composite spectra.*

Star	Effective Temperature (K)	Angular diameter milliarcsec
α Boo	4362	21.12
γ Dra	3986	10.17
α Cet	3745	12.77
γ Cru	3626	26.14
μ UMa	3735	8.32

*This table can be found in the AAS CD-ROM Series, Vol. 7, 1996.

measured spectral points were ~3%–5% in molecular lines.

As in Paper IV, we have substituted the best-fitting Engelke (1992) function for noisy LRS, 16–24 μm CGS3, and/or 16–35 μm *KAO* data to provide meaningful extrapolations of our new composites out to 35 μm. This analytic approximation to real stellar continua is derived assuming that the dominant source of infrared continuum opacity in these cool giant stars is H⁻ free-free (cf. Engelke 1992). There is only one essential input to the shape of an Engelke function, namely the effective temperature, which we fixed by reference to the literature (see Tables 2, 3, and the AAS CD-ROM Series). The normalizing scale factors for these functions, namely their angular subtenses, are determined by the fit of the Engelke function shape to our composite spectra.

We document the full calibrational information for these new composites (see Table 4 and the CD-ROM), namely, date of assembly (i.e., the version of this spectrum); details of the photometry used to calibrate the composite radiometrically including the FWHM of the relevant passbands and their effective wavelengths for the Vega spectrum and for the star in question, and the monochromatic flux densities; all archival spectral fragments, with total spectral ranges, ranges actually utilized, and average resolving power over that spectral range (expressed as the resolving power, $\lambda/\Delta\lambda$). We had access to adequate photometry to assemble the composites for α Boo, γ Dra, μ UMa, and γ Cru by precisely the same technique used for that of α Tau (Paper II) and the 1.2–35 μm spectra detailed in Paper IV. For α Cet we lacked any traceable photometry in characterized passbands in the 10 μm window and were, therefore, obliged to assemble this star's composite using the "end-to-end" method used in Paper VI for the composite spectrum of α^1 Cen.

The star μ UMa is now designated as a new suspected variable (NSV 4829) by Kholopov *et al.* (1992), although details are minimal. Hoffleit & Warren (1991) indicate it to be a spectroscopic binary, possibly an eclipsing variable, with visual amplitude about 0.3 mag. Examination of the infrared literature (Gezari *et al.* 1993) does not suggest infrared variation above a few hundredths of magnitude, after allowance for the diverse zero points of the references cited therein, although Sinton & Tittemore (1984) indicate qualitatively that they saw some variation at M. Consequently, we have retained this star as a secondary standard because of its popularity as an infrared calibrator, due as much to its northerly location as to its mid-infrared brightness.

In addition to the photometry used for the actual assembly of composites (the filled squares in Fig. 1), we sometimes have other photometry in well-characterized passbands that can be used to validate the spectra, precisely because it was unused by our procedures. Any such points are distinguished, in Fig. 1, by open squares (ground-based data) or by open triangles (*IRAS* data, similarly not used in composite assembly). All photometry points are plotted at their isophotal wavelengths for these stellar spectra. These validating data points are as follows. For α Boo we have: narrowband Jn (Selby *et al.* 1988; Hammersley 1995, described in Paper VIII); UKIRT broad *N*-band (10 μm) and *Q*-band (20 μm) points (too wide to be integrated over the CGS3 10/20 μm fragments but valid post factor; and the *IRAS* FSS flux densities at 12 and 25 μm. For γ Dra, these are narrowband Jn (Selby *et al.* 1988; Hammersley 1995) and broadband Tenerife J (Hammersley 1995); a UKIRT *Q*-band point; and *IRAS* FSS points. For the other three stars, we have only *IRAS* flux densities as external checks of the composites. In all five cases, these additional photometry values confirm the accuracy of the new composites at the 1σ level or better.

We prefer to provide pristine data whenever possible, rather than to regrid each composite to some equally spaced or common wavelength scale. Each composite (on the CD-ROM), therefore, has a different set of wavelengths. We tabulate: wavelength; monochromatic flux density (F_λ in units of W cm^{-2} μm^{-1}); total uncertainty (also in units of W cm^{-2} μm^{-1}) associated with this value of F_λ; local bias; and global bias. For most applications, "total uncertainty" is the error term most appropriate to use. It is the standard deviation of the spectral irradiance and includes the local and global biases. Local and global biases are tabulated as percentages of the irradiance; their corresponding absolute quantities are already included in the total uncertainty. The global bias does not contribute error to flux ratios or color measurements, and may be removed (in the root-sum-square sense) from the total error.

3. COMPARISON WITH KURUCZ MODEL ATMOSPHERES

De Jager & Nieuwehuisen (1987) tabulate statistical relations between effective temperature and bolometric luminosity for all spectral types, assigning algebraic variables, that can be interpolated, to the qualitative descriptors of "spectral class" and "luminosity class." Following the approach and work of de Jager & Nieuwehuisen, Cohen (unpublished) has constructed similar tables that correspond to stellar mass and radius, using values drawn from the literature, whence a derivative relation between gravity and spectral type was obtained. Adopting solar metallicities, appropriate effective temperatures, and these gravities (corresponding solely to the spectral types of our stars), we have extracted theoretical spectra from the Kurucz grid. To provide a generic model for each selected set of values for temperature and gravity, we interpolated bilinearly in log T_{eff} and log g within the Kurucz archive.

Each pair of model and composite spectra was then convolved with a Gaussian and the model regridded to the same wavelength scale as the corresponding composite. We then fitted the complete emergent spectrum from the model atmosphere to the composite, omitting only the region 7.43–11.25
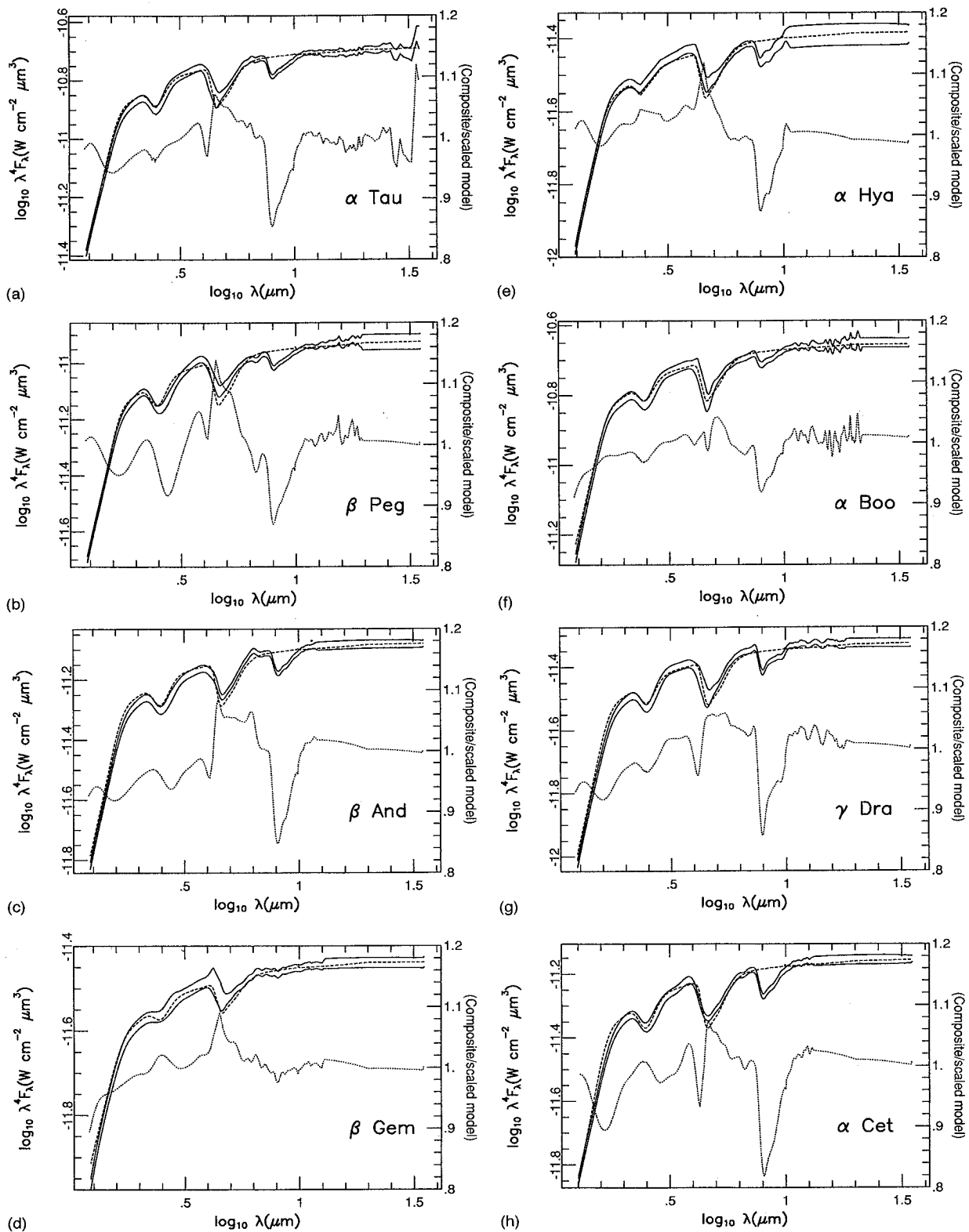
FIG. 2. Eight 1.2–35 μm composites, smoothed by a Gaussian with FWHM of 0.3 μm, showing their $\pm 1\sigma$ ranges (pairs of solid lines), compared with the identically smoothed relevant Kurucz models (short dashed lines), scaled optimally to match each composite spectrum, excluding only the region of the SiO fundamental (log $\lambda \sim 0.90$). (These curves are to be read against the left-hand axes.) The major CO bands occur at log $\lambda \sim 0.67$ (fundamental) and log $\lambda \sim 0.36$ (first overtone) in these plots. The ratios of these smoothed spectra are also plotted in these figures (the dotted curves), in the form of composite divided by scaled model. These dotted ratio curves are associated with the right-hand axes. Note the SiO ratio absorption due to the absence of the lines of this fundamental band (log $\lambda \sim 0.90$) from the grid of models, and the apparent "emissions" in the CO fundamental (log $\lambda \sim 0.67$), where the models' bands are too deep. (a) α Tau, (b) β Peg, (c) β And, (d) β Gem, (e) α Hya, (f) α Boo, (g) γ Dra, (h) α Cet.

TABLE 3. Fundamental parameters adopted for the generic Kurucz models.*

Star	Spectral Type	T_{eff}	$\log g$
α Tau	K5III	3898	2.0
β Peg	M2.5II-III	3600	1.4
β And	M0III	3839	1.5
β Gem	K0III	4844	2.5
α Hya	K3II-III	4141	2.2
α Boo	K1III	4362	2.4
γ Dra	K5III	3986	2.0
α Cet	M1.5III	3745	1.3

*This tale can be found in the AAS CD-ROM Series, Vol. 7, 1996.

μm, where the SiO fundamental is apparent in the observations but lacking in the Kurucz models. The "fit" was accomplished simply by treating the smoothed model and the smoothed composite as two independent spectral fragments that we wished to "splice." This procedure (described in detail in Paper II) involves χ^2 minimization of the sum-squared differences between the two spectral shapes, taking into account the variances of the observed points. The method provides the overall optimal scale factor for the model, and hence provides a value for the angular diameter. The results showed minimal sensitivity to sensible values of the FWHM used for the smoothing (i.e., in the range 0.1–0.3 μm).

Figure 2 illustrates the results of these direct comparisons, where we present the ratios of eight of our twelve composites (those with fullest wavelength coverage) to the optimally-scaled relevant Kurucz models. The fundamental parameters we used for the eight stars presented in these figures are summarized in Table 3. (The four spectra not shown present similar comparisons though the quality of fit is higher when we have a broader spectral range in the observations.) Apart from the SiO fundamental region ($\lambda\sim8.0$ μm), the models fit well, and the ratio spectra are essentially featureless (allowing for the 1σ absolute uncertainties in our spectra), except for deviations of order 10% through the CO fundamental ($\lambda\sim4.7$ μm) and occasional, smaller, more ambiguous, features in the CO first overtone bands ($\lambda\sim2.3$ μm). We conclude that the Kurucz models provide good predictors of stellar spectral energy distributions for these cool giants, at better than the $\pm2\%$–3% level outside the major CO and SiO absorption features, and about 5%–10% in the CO bands. We recognize that α Boo is anomalous for its spectral type by virtue of its metal-poor character, yet this appears predominantly to affect the strong bands and not the less heavily blanketed regions where the spectrum approaches the true continuum.

The discrepancies in CO might arise for a number of reasons, including our use of generic, as opposed to customized, models for these individual stars, Kurucz's use of comparatively old CO line strengths (i.e., Kirby-Docken & Liu 1978), and the omission of H_2O opacity in the Kurucz models. Further investigation will be needed to sort this out. It is interesting to note that there is no clear tendency for stars of lower temperature to have systematically greater deviations

TABLE 4. "Header" information accompanying new α Boo composite.*

12-21-95 OBSERVED SPECTRUM OF ALPHA BOOTIS
α Boo photometry file: photometry actually used to construct the spectrum

Name	FWHM (μm)	Mag.±Unc.	Eff Wvl (Vega) (μm)	Eff Wvl (star) (μm)	F_λ W cm^{-2} μm^{-1}	Source
Kn	0.0488	-3.07±0.01	2.208	2.205	6.69E-13	Selby,Hammersley
Ln	0.1443	-3.15±0.01	3.782	3.762	9.35E-14	Selby,Hammersley
M	0.6677	-2.97±0.02	4.758	4.738	3.24E-14	Strecker *et al.* 1979
UKIRT87	0.8611	-3.13±0.01	8.770	8.779	3.43E-15	UKIRT Service data
UKIRT98	0.9455	-3.16±0.01	9.843	9.828	2.23E-15	UKIRT Service data
UKIRT11	1.1198	-3.16±0.01	11.641	11.639	1.15E-15	UKIRT Service data
UKIRT12	1.1782	-3.19±0.01	12.432	12.427	9.13E-16	UKIRT Service data

This UKIRT filter set represents a series of narrowband 10 μm passbands provided in common to UKIRT, Univ. Minnesota, and IRTF for "silicate" work. The "11" filter is centered near 11.7 μm, the"12" filter is centered near 12.5 μm.
Spectral fragments and portions of these actually used in observed spectrum ("used" may include combination with other data where overlaps occur)

Fragment	Reference	Total range (μm)	Start and stop wavelengths (μm)	Average resolving power
NIR	1	1.22–5.70	1.22–5.58	50
KAO	2	3.65–9.39	4.44–8.99	150
8–13	3	7.65–13.43	7.65–13.43	55
LRS	4	7.80–22.70	9.30–21.90	30
LONG	5	15.73–23.85	15.73–23.85	73
VLONG	6	1.25–35.00	21.80–35.00	–

References:

● 1. Strecker, Erickson, & Witteborn 1979, Ap.J. Suppl., 41, 501.

● 2. FOGS data of May 11, 1992 KAO flight [α Boo/α Lyr], and HIFOGS data of April 14, 1995 KAO flight [α Boo/α Lyr].

● 3. FOGS Mt Lemmon data of Feb. 24, 1992 [α Boo/α Lyr], CGS3 UKIRT data of May 24 and 29, 1991 [α Boo/β Peg], August 12, 1995 [α Boo/β Peg] and [α Boo/β And]. The CGS3 spectra have the greatest weight in this combined data set.

● 4. LRS raw data extracted from the new Groningen IRAS database and recalibrated with "LRSCAL" routine in "GIPSY" package.

● 5. 20 μm UKIRT CGS3 data of May 24/25, 1991 for [α Boo/β Peg].

● 6. Engelke Fn. used for T=4362K (see Blackwell, Lynas-Gray, & Petford 1991, A&A, 245, 567) and angular diameter=20.430 mas; we rescaled this to 21.12 mas. This Engelke Function was locked to the photometrically scaled combination of 8--13 and LRS spectra by splicing and used to replace the observations beyond 21.80 μm. We applied an estimated uncertainty in EFn. of 2.4%, allowing for the change in shape of the EFn. for a temperature uncertainty of 100K at this effective temperature.
INFORMATION ON SPLICES AND BIASES INCURRED

Process	Factor determined	±Bias (%)
NIR cf. photometry	1.003	0.87
813 cf. photometry	1.031	0.45
LRS blue/red bias	–	0.03
LRS splice to 813	0.950	0.02
KAO joint splice to NIR and merged 813/LRS	0.862	0.41
LONG splice to merged 813/LRS	1.124	0.66
Engelke Fn. splice to combined 813/LRS/LONG	1.017	0.40

*Actual spectra for other stars can be found in the AAS CD-ROM Series, Vol. 7, 1996.

from expectation, in spite of the absence of H_2O lines from the Kurucz models. In the near future, we plan a much more extensive investigation of the influence of all the H_2O, CO, and SiO lines that must be present in these giants on their emergent spectra. The overriding impression conveyed by Fig. 2, however, is of the strong predictive power of these models in representing these observed spectra.

4. STELLAR ANGULAR DIAMETERS

Table 5 (this table can also be found in the AAS CD-ROM Series, Vol. 7, 1996) summarizes four estimates of angular diameter for these stars: (i) from the multiplicative scale of the best-fitting Kurucz model appropriate to each star (as just described); (ii) from our Engelke approximations; (iii) from the independent work of Blackwell *et al.* (1990), Blackwell *et al.* (1991) using the MARCS model atmosphere code and a different absolute calibration for Vega

TABLE 5. Comparison of derived angular diameters with measured values.*

Star	Kurucz model	Our Engelke function	Blackwell et al. IRFM	Observed	Reference
α Tau	20.92	21.32	20.63	20.88	Ridgway et al. 1982
	±0.21	±0.58	±0.41	±0.10	
β Peg	16.49	16.98	16.73	16.75	Di Benedetto & Rabbia 1987
	±0.16	±0.51	±0.33	±0.24	
β And	13.47	13.71	13.22	13.81	Mozurkewich et al. 1991
	±0.13	±0.37	±0.26	±0.11	
β Gem	8.01	8.07	7.87	8.03	Mozurkewich et al. 1991
	±0.08	±0.17	±0.16	±0.08	
α Boo	20.76	21.12	20.43	20.95	Di Benedetto & Foy 1986
	±0.21	±0.51	±0.41	±0.20	
γ Dra	10.04	10.17	10.00	10.13	Di Benedetto & Rabbia 1987
	±0.10	±0.27	±0.20	±0.24	
α Cet	12.52	12.66	12.64	13.23	Mozurkewich et al. 1991
	±0.13	±0.36	±0.25	±0.20	
γ Cru	25.49	26.14	–	–	
	±0.25	±0.86			
α Hya	9.21	9.27	–	–	
	±0.09	±0.24			
α TrA	9.51	9.55	–	–	
	±0.10	±0.26			
μ UMa	8.16	8.32	–	–	
	±0.08	±0.28			
ε Car	12.39	12.67	–	–	
	±0.12	±0.33			

*This table can be found in the AAS CD-ROM Series, Vol. 7, 1996.

than our own, or Blackwell & Lynas-Gray (1994), who revised their earlier results to use the Kurucz model grid and adopted our absolute calibration of the Selby narrowbands (Paper I); and (iv) from Michelson intensity interferometry. For the latter, we have used the "true" (limb-darkened) angular diameters (as opposed to those based on interpretation of the observed visibility fringes with the "uniform diameter" assumption). Details of the calculations used to convert observed to true angular diameters are presented by Di Benedetto & Rabbia (1987), Mozurkewich et al. (1991), and in the more recent summary by Di Benedetto (1993). For α Tau, there is also an extensive series of measurements based upon lunar occultations (see White & Feierman 1987) with the best weighted value for this star being 20.88 mas (Ridgway et al. 1982). (In the lower part of Table 5, we have included the five stars apparently without direct observations, or IRFM-based estimates of diameter.) There is good accord between all four estimates for the seven stars for which all this information is available. The existence of such an accord makes a profound statement because each estimate is based on a very different spectral region. Our match to Kurucz models assesses the quality of fit over each entire composite (excluding the SiO fundamental), but this effectively assigns greatest weight to the shorter wavelengths (below ~7.5 μm), where our total uncertainties are relatively small. By contrast, our Engelke approximations are fitted to the observed spectra longward of the SiO fundamental, typically beyond 12 μm. Blackwell and colleagues treat only narrowband photometry in the 1.2–3.8 μm region. Yet all these methodologies agree with the direct observations within the stated errors, and the technique of matching generic Kurucz models to composites provides meaningful diameters and formal uncertainties in these diameters.

The third column in Table 5 presents the most recent determination of angular diameter by Blackwell and colleagues for each of these stars. This corresponds to the Blackwell et al. (1991) paper for all stars except β Gem, for which Blackwell & Lynas-Gray (1994) provide a new value of 8.03 mas with a methodology that is closest to our own (Kurucz

models; our calibration of the Selby passbands). This value is essentially identical to our own diameter (8.01 mas). Unfortunately, these authors have not published similarly recalibrated diameters for the other stars in Table 5. It is difficult to make accurate estimates of what values they would have obtained by application of their most recent method but, based on β Gem, their diameters would have been quite close to our values.

We note from Table 5 that the Kurucz models lead to systematically smaller angular diameters than indicated by the observations. We can speculate on possible causes of this phenomenon but we cannot fully account for it in the present paper. Several factors may contribute. First, the particular technique used here is designed to treat stars as though we lacked individual knowledge of their fundamental parameters, including elemental and isotopic abundances (in readiness for application of the generic "template" scheme in the future). Perhaps, in this manner, or through our effective temperature-spectral class transformation, we have systematically misrepresented the actual stars. Second, perhaps our attempt to fit the entire observable spectral region, without the SiO fundamental, has made our result more vulnerable to any inadequacies in the representation of the absorption strengths of the myriad molecular lines. (Recall in particular that the Kurucz and MARCS models do not include the potentially important H_2O opacity.) Use of a different scheme which weights the relative continuum portions of the spectrum more heavily might lead to more secure diameters. However, even this is unclear since the fluxes in these "continuum" regions are affected in reality both by a veil of molecular lines and by the brighter true continuum levels which arise when deeper atmospheric layers are heated by line blanketing. The Selby narrowband filters used to support the IRFM have isophotal wavelengths close to 1.25, 2.21, and 3.78 μm (logarithmic values of 0.10, 0.34, 0.58). These tend to correspond to local maxima close to unity in the ratio plots shown in Fig. 2. Therefore, basing our scaling of models on the fluxes at these wavelengths might improve the agreement with the observations.

The diameters implied by the Engelke approximations are generally bigger than those from using real models. This arises because Engelke functions are essentially Rayleigh–Jeans in character in the domain in which we employ them, whereas true model spectra decline more slowly with increasing wavelength. Therefore, to match the level of a given observed spectrum, one requires larger scale factors for Engelke functions.

It is worth emphasizing that the diameters derived from both the Kurucz and MARCS models generally accord, at the 1σ level, with the observed diameters. This level of agreement implies discrepancies in diameter at only the 1% level, yet Blackwell & Lynas-Gray (1994) estimated conservative uncertainties in diameters derived by the IRFM of 4%. It is interesting that neither model grid reproduces the observed subtense of α Cet, but one must recall that angular diameters of resolved stars depend on limb darkening corrections to derive the "true" diameter from the observed. Such corrections might plausibly be suspect on very cool giants such as α Cet. An informative discussion of the complexity
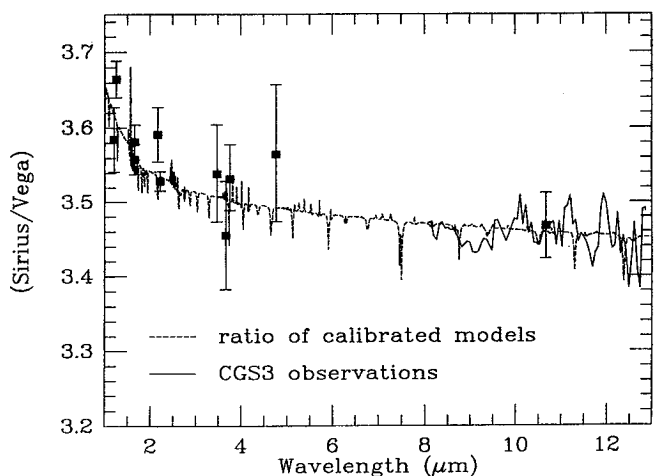
FIG. 3. Ratio of calibrated models of Sirius and Vega (short dashed line), compared with CGS3 direct spectral observations (solid line), and with the measured broad and narrowband ratios (filled squares with $\pm 1\sigma$ error bars) in well-characterized infrared photometric bandpasses.
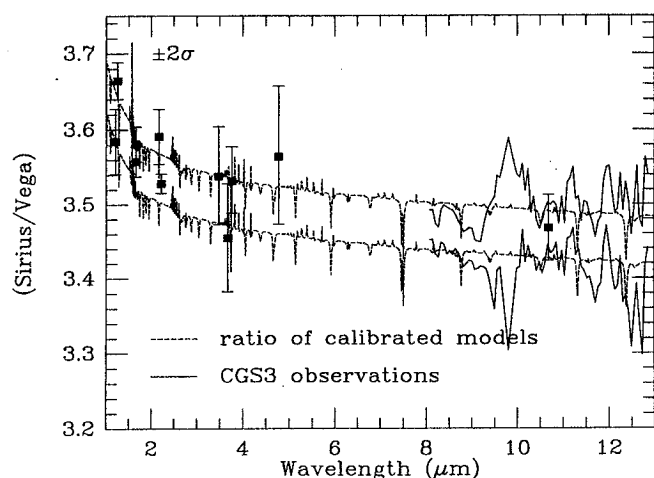
FIG. 4. As for Fig. 3, but now combining direct and indirect CGS3 spectroscopy of Sirius/Vega, and illustrating the $\pm 2\sigma$ bounds on the ratio of the model spectra.

of limb-darkening in cool photospheres may be found in Scholtz & Takeda (1987).

Finally, for γ Cru, our angular diameter is quite different from the 41.1 mas cited by Judge & Stencel (1991). However, their value was an indirect one, based upon adopting colors similar to those of other very cool M giants and applying relations due to Barnes *et al.* (1978) between color and visual surface flux (Stencel 1996; cf. Judge & Stencel 1991, Appendix A, Sec. 2, last sentence).

5. THE SPECTRAL RATIO OF SIRIUS/VEGA

The derivation of plausible angular diameters from our composites provides external validation of their accuracies. This, in turn, vindicates the procedures we have devised to assemble composite spectra. The derivation (Paper VI) of an angular diameter for α^1 Cen, that is consistent with the literature for that star, is a further indirect check on the adopted, calibrated model for Sirius. As a final cross check on the overall scheme we have sought data not used in Paper I on the ratio of Sirius to Vega. Two kinds of data are of value: independent photometric measurements of Sirius compared with Vega; and the ratio of their spectra.

Our calibration of the Kurucz Sirius model relative to the calibrated model for Vega (Paper I) was based upon the bolometry of Cohen & Barlow, published by Deacon (1991). Therefore, we sought other well-characterized photometric systems for which the difference in magnitude between these hot stars has been measured. We require detailed cold-scanned filter transmission profiles for these systems, and we have applied an atmosphere appropriate to each site (cf. Paper I). Of particular value are data by Carter (1996: detailed in Paper VIII) in the *SAAO JHKL* system [as characterized for us by Glass (private communication)], and by Hammersley (1995: *JHK*; to be represented in detail in Paper VIII) and Alonso *et al.* (1994: *JHKL'*) in the Tenerife broadband InSb passbands. The *JHK* data of Alonso *et al.* are already included in Hammersley's reanalysis of the entire photomet-

ric archive of the Telescopio Carlos Sanchez (Paper VIII) so only these authors' *L'* result is separately represented here. Additional photometry can be found in Sinton & Tittemore (1984) using *L'* and *M* passbands which, from their descriptions, are identical with the UKIRT bolometer passbands of the same name that we calibrated in Paper I (although Sinton and Tittemore's measurements were never used in Paper I). We emphasize that we have taken great pains to avoid circularity: we do not use our expectation for Sirius' magnitudes in these passbands from a recalibration of the authors' systems, but focus strictly on the observed differences in magnitude as measured by these authors. Figure 3 illustrates the ratios equivalent to each of these magnitude differences between Sirius and Vega. Filled squares represent the photometry with $\pm 1\sigma$ error bars, defined as the root-sum-square of the observed magnitude uncertainties of these two stars, in each passband. Points are plotted at their isophotal wavelengths (almost identical in these bands for Sirius and Vega: cf. Paper I). The longest wavelength point plotted in Fig. 3 and 4 is the high precision measurement made by *IRAS* at 12 μm (from Table VI.C.3 in the *IRAS* Explanatory Supplement 1988).

We wish to make a comparison of our adopted ratio of the two model spectra, and to assign meaningful uncertainties to their ratio. The relevant uncertainty for the spectral ratio of Sirius to Vega is the uncorrelated error, rather than the underpinning 1.45% absolute uncertainty in Vega's calibration which is directly transferred, as a bias (a correlated uncertainty), when we calibrated Sirius relative to Vega. If we assign uncertainties of $\pm 0.01^m$ to each of Deacon's magnitudes, then the root-sum-square of these random errors with the small bias associated with locking the Sirius model to the expected photometry of Deacon, yields a conservative estimate of $\pm 0.5\%$. Figure 4 compares this photometry with the $\pm 2\sigma$ bounds in the mean ratio of our adopted calibrated spectra for these stars (short dashed lines). The photometry points appear to follow the upward trend (with decreasing wavelength) in the models' spectral ratio very well. This is
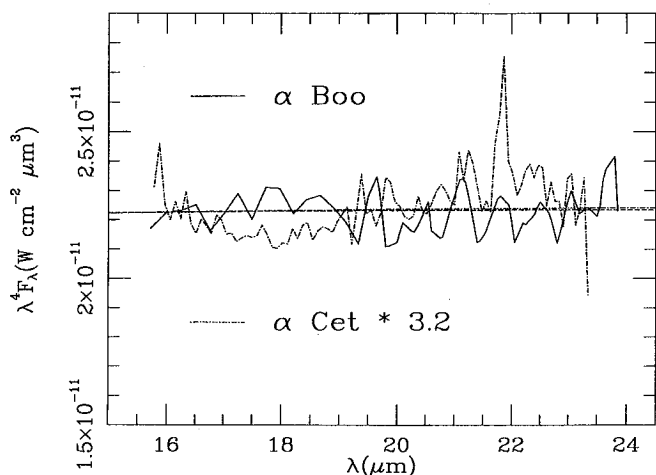
FIG. 5. Further evidence for the Rayleigh–Jeans character of cool stellar spectra in the form of spectral "flatness" in $(\lambda, \lambda^4 F_\lambda)$ space. UKIRT CGS3 16–24 μm spectra for α Boo (unscaled, solid line) and α Cet (scaled by a factor 3.2, dash-dot line) are compared with their relevant Engelke approximations (dashed lines across the middle of the plot). That for α Boo appears slightly above that for α Cet.
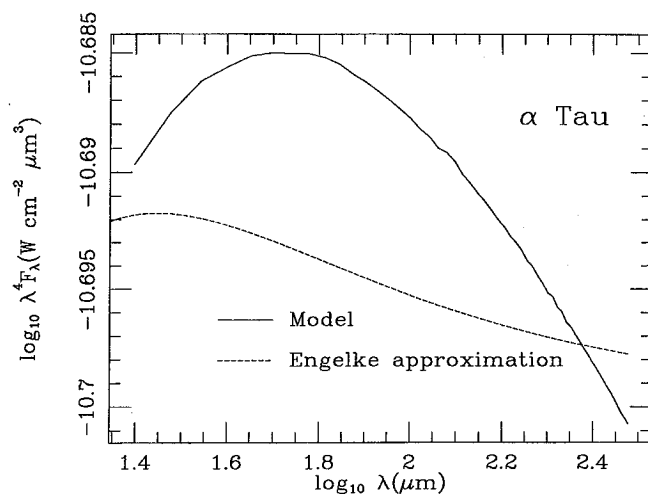

FIG. 6. Far-infrared model continuum extrapolation (solid line) of our α Tau composite, compared with the extrapolated Engelke approximation (short dashed line) for this star. The maximum difference between these two spectra occurs near 65 μm, where it attains almost 2%.

entirely due to differences in the two adopted stellar effective temperatures.

What observational spectroscopic evidence can we adduce in support of our models' ratio? There are two kinds of measurement to discuss, because it is a challenging observation to secure spectra of Sirius and Vega in a single night. Given data on the two stars in one night, one can construct the direct spectral ratio. The second, indirect, measurement of spectral ratio that we consider is formed by use of intermediate stars, so that one compares an airmass-matched ratio (cf. Papers II, V) of Sirius to a bright star, and of Vega to the same bright star, also matched in the airmasses of observation. The indirect method offers the advantage of being able to choose good bright intermediaries and to secure close matches in airmass, at the cost of added noise in the eventual ratio of Sirius to Vega, attendant on the products or quotients of these intermediate ratio spectra.

We have found one direct measurement of Sirius to Vega from the UKIRT archives. This is constructed from 10 μm spectra taken with the CGS3 spectrometer, by Skinner and Sylvester on 1992 October 4, and kindly furnished for our use by Sylvester (1996). The two stars were not closely matched in airmass (Vega $z = 1.29$; Sirius $z = 1.55$). Consequently, the short-wavelength edge was lost to water vapor differences and the 9.6 μm telluric ozone feature was uncanceled. This necessitated deletion of the affected data (7.5–7.7 and 9.75–9.9 μm). The resulting spectrum was normalized using photometry from Deacon (1991) in the UKIRT 8.7 μm "narrowband" filter. Figure 3 presents this direct spectral ratio, as the simplest comparison we can make with the models' ratio.

To enhance signal to noise, we needed to secure additional indirect spectral ratios, so we sought airmass matching with bright intermediaries. Two such indirect routes are available to us from the UKIRT CGS3 archives. One involves the quotient of ratios of spectra, [β Peg/α Lyr] (1995

August 12) and [β Peg/α Tau] (1993 November 4 and 5), from which we derive an estimate of the spectral ratio [α Tau/α Lyr]. The second similarly involves [β And/α Lyr] (1995 August 11 and 12) and [β And/α Tau] (1993 August 28), whose quotient gives another estimate of [α Tau/α Lyr]. We combined these two ratio spectra (with inverse-variance weighting) to yield a cleaner [α Tau/α Lyr], which we divided by our published ratio of [α Tau/α CMa] (from 1991 November 9: Fig. 4 of Paper III), to create [α CMa/α Lyr]. Finally, we combined this indirect ratio (which has broader wavelength coverage than the direct method because of the close matching in airmasses of the quotient spectra) with the direct approach, using inverse variance weighting. Essentially the same spectral ratio results as from the direct measurement alone, but now it is seen with higher signal to noise and over a larger and more completely sampled wavelength interval. The resulting ratio spectrum appears in Fig. 4, where we have indicated the $\pm 2\sigma$ bounds on this observed spectrum, exactly as shown for the ratio of model spectra. The two $\pm 2\sigma$ swathes (model and CGS3) overlap significantly.

Therefore, we conclude that both independent photometry and spectroscopy support the ratio of our two, independent, adopted models for the spectra of Sirius and Vega.

6. THE BEHAVIOR OF REAL GIANT STARS FROM 10 TO 35 μm

The agreement between cols. (1) and (2) of Table 5 suggests that the simplistic Engelke function is a reasonable approximation to the general shape of emergent spectra predicted by fully detailed model atmosphere calculations. Closer inspection reveals that the diameter implied by the Engelke approximations is invariably larger than that from matching to real models. This happens because Engelke functions decline slightly faster with wavelength than model spectra, and therefore require slightly greater multipliers to match a given observed spectrum. What of real stars?

Only two normal giant stars, α Tau and γ Cru, were observed by Glaccum (1990) from the *KAO*, and these spectral fragments owe their shapes to standard planetary absolute calibration techniques (Paper II; Moseley *et al.* 1989). These two stars do seem to behave in a Rayleigh–Jeans fashion once the spectrum rises out of the strong SiO fundamental absorption; i.e., in $\lambda^4 F_\lambda$ space, their observed spectra are essentially independent of wavelength beyond about 12 μm. Additional support for the observed "flatness" of real stellar spectra in this space (Figs. 1 and 2) comes from our CGS3 20 μm spectra taken at the UKIRT and, to a lesser extent (due to the noise at the longest wavelengths), from the LRS too (cf. for α Tau in Fig. 11 and 12 of Papers II; for γ Cru, Fig. 5, and β And, Fig. 6, both in Paper IV). In the present paper, we adduce additional evidence for the Rayleigh–Jeans nature of real stellar spectra from 20 μm CGS3 spectra of α Boo and α Cet. These are compared, in Fig. 5, with the relevant Engelke approximations. The spectral "flatness" is emphasized by these direct plots of the calibrated stellar spectra in $\lambda^4 F_\lambda$ space.

7. SYNTHESIZING IRAS 12/25 μm FLUX DENSITIES

We hoped further to probe this apparent and persistent discrepancy between the long-wavelength (beyond ~ 12 μm) behavior of real and model stars, by comparing our composite spectra with *IRAS* observations. Every composite is fundamentally built from observations based on our model spectra for Sirius and Vega. Therefore, we would expect to conclude in favor of the same "recalibration" factors for *IRAS* flux densities deduced from photometry alone in Paper I, by use of *IRAS* flux densities synthesized from our composites, unless real stars deviated significantly from Rayleigh–Jeans slopes. The procedure is straightforward, requiring only the integration of the *IRAS* system response functions for the 12 and 25 μm passbands over our spectral composites, and direct comparison with the *IRAS* in-band fluxes, and the flux densities derived from these upon division by the bandwidths (cf. Paper I).

Table 6 (also found in the AAS-CD-ROM Series, Vol. 7, 1996) summarizes the results of these direct comparisons with the *IRAS* Faint Source Survey (Moshir *et al.* 1992), reputedly of higher quality than the *IRAS* Point Source Catalog (1988: hereafter referred to as PSC) fluxes, and with the PSC itself. Table 6 incorporates both the uncertainties that attend our derived fluxes and those inherent in the *IRAS* measurements ("RELUNC" quantities in these catalogs). The comparison suggests that these *IRAS* point source products overestimate 12 and 25 μm flux densities by statistically the same amount in the PSC and the FSS, namely, by 4.1% at 12

and by 5.7% at 25 μm. From this we conclude that our spectral composites, based on the calibrated spectra of Sirius and Vega (Paper I), represent self-consistent products because these factors for *IRAS*'s calibration, derived here from cool stellar spectra (0.96±0.01 and 0.94±0.01), are in accord (at the 1σ level) with those determined purely from our basis models for Sirius and Vega (12 μm: 0.98±0.01; 25: 0.94±0.02). It is also tempting to conclude that, in the ensemble average, *IRAS* measurements vindicate the essentially Rayleigh–Jeans character of the infrared photospheric emission from these cool giants in the 7–35 μm range, although the actual *IRAS* uncertainties on any star are too large to reach this conclusion for an individual object.

8. EXTRAPOLATION OF COMPOSITES TO 300 μm

The 35 μm limit of our standard composite spectra does not afford the same test with longer wavelength *IRAS* data. Consequently, we have adopted the emergent spectral shapes of a grid of mid- to far-infrared continuum models of red giant branch stars, computed as described below. We interpolated in this grid to provide a model that matched the correct effective temperature for each composite (and we assumed the red giant branch gravities interpolated were correct for our observed giants). The attributes of the giants come from VandenBerg & Laskarides (1987) and are close to the expected gravities for our giants. By fitting these shapes to the *observed portions* of composites, longward of the SiO fundamental's influence, but shortward of the wavelength where we chose to replace noisy data by Engelke functions, we created best-fitting extensions of each composite.

In order to obtain representative effective temperature-log(gravity) $(T_{\rm eff}, \log g)$ combinations for the late-K and early-M giant branch stars of the disk in our observed sample, we adopted the theoretical red giant branch tracks computed by VandenBerg & Laskarides (1987). We chose the particular track with the following model parameters: $\mathcal{M}/\mathcal{M}_\odot = 1.3$; $Y = 0.25$; $Z = 0.0169$; [M/H] $= 0.0$.

Stellar evolution models with these parameters have an age of 5.28 Gyr at the He flash and, thus, should be reasonably representative of evolved stars of the disk. To obtain the $(T_{\rm eff}, \log g)$ needed for the stellar model atmosphere calculations, we selected three combinations of $(T_{\rm eff}, \log g)$, spaced by 500 K, on the aforementioned VandenBerg & Laskarides track: (4500,2.86), (4000,1.87), and (3500,0.975).

To obtain a model which might be appropriate for the hottest star in our sample, β Gem, we adopted the specific parameters of $T_{\rm eff} = 4844$ K and $\log g = 2.24$, which are in excellent agreement with the analyses of this star by Blackwell & Lynas-Gray (1994), Di Benedetto (1993), and Ruland *et al.* (1980).

To obtain the temperature vs. continuum optical depth at 1 μm relations $[T(\tau_{1 \ \mu{\rm m}}^c)]$, needed to compute emergent fluxes for our four desired models, we began with published model grids and proceeded in the following fashion for each of the desired models:

(1) the temperature–pressure relation of the grid model

TABLE 6. Ratios of *IRAS* flux densities synthesized by integration of the *IRAS* passbands over our observed composite spectra (12,25 μm), extrapolated by model atmospheres (60,100 μm), to those actually observed by *IRAS*.*

IRAS data	12 μm	σ	25 μm	σ	60 μm	σ	100 μm	σ
FSS	0.961	0.012	0.946	0.013	0.997	0.015	1.038	0.040
PSC	0.961	0.010	0.943	0.010	0.985	0.029	1.015	0.026

*This table can be found in the AAS CD-ROM Series, Vol. 7, 1996.

nearest in T_{eff} and $\log g$ to the desired model was used to obtain the grid model's $T(\tau_1^c {}_{\mu m})$;

(2) the grid model's $T(\tau_1^c {}_{\mu m})$ relation was then scaled by the ratio T_{eff}(desired)/T_{eff}(grid model). The validity of this procedure over moderate ranges in T_{eff} has been demonstrated by Carbon & Gingerich (1969) and Gustafsson *et al.* (1975);

(3) and, finally, using the resultant $T(\tau_1^c {}_{\mu m})$, the equation of hydrostatic equilibrium was reintegrated using the $\log g$ of the desired model.

All the calculations were carried out using the set of solar abundances adopted by the authors of the respective model grids.

For the three coolest models, (4500,2.86), (400,1.87), and (3500,0.975), we interpolated in the model atmosphere grid published by Brown *et al.* (1989). For the β Gem model, (4844,2.24), we interpolated in Kurucz's (1991, 1993) model grid to obtain the required T–P relation. For each of the four models, we computed continuum spectral energy distributions at 101 wavelengths from 1.0 to 300 μm using the SOURCE model atmosphere program described in Carbon *et al.* (1982). For *ISO* purposes, we created products gridded every 5 μm from 25 to 300 μm to supplement and extend our absolute calibrated composites out to the longest wavelengths relevant to *ISO*.

We assessed uncertainties in these extrapolations based on the recent study of the sensitivity of far-infrared continua to fundamental stellar parameters by van der Blieck *et al.* (1996). Explicitly, at 100 μm, these are ~2% (corresponding to ±100 K in effective temperature), ~0.2% (±0.3 in $\log g$), and ≤1% (±0.2 in metallicity). In fact, as these authors point out, errors in gravity are even greater for late-type giants than for ensembles of warmer stars, typically attaining ±0.5 in $\log g$. Van Blieck *et al.* (1996) also simulated chromospheres and considered the influence of circumstellar dust. We examined their estimates for uncertainties in far-infrared flux due to errors in fundamental parameters, in temperature structure, and other causes, and adopted 4.8% as typical for the root-sum-square combination of all these components for the mid-G to early-M giants they considered. To these we have appended an extra 3% to account for the typical expected contributions to the spectra of molecular line blanketing due to the copious lines of water vapor, CO, and SiO, and their isotopes.

9. SYNTHESIZING IRAS 60/100 μm FLUX DENSITIES

These extrapolated composites permit integration over the 60 and 100 μm *IRAS* bands. Table 6 presents the results of direct comparison of long-wavelength flux densities synthesized from our spectra with those measured by *IRAS*. In spite of the rather larger relative uncertainties, "RELUNCs," associated with the *IRAS* long-wavelength measurements we can, nevertheless, determine from this ensemble of composites that *IRAS* measurements are consistent with our calibrated observed spectra, extrapolated through theoretical model atmospheres.

It is, perhaps, also of interest to examine the long-wavelength quality of the simplistic Engelke approximations.

The absolute difference in emergent spectra of these giants, between their best-fit Engelke approximations and our grid of far-infrared continua, is always small. In fact, as Fig. 6 illustrates, for α Tau it amounts to a mere 2% over the range 25–200 μm. For the set of 12 composites now available, this maximum difference between Engelke approximations and model continua lies in the range 2%–5%, and always occurs between 60 and 70 μm. As a further test, we also continuedthe same Engelke functions that best fitted each composite (see Papers IV, VI, and this paper) to wavelengths long enough to synthesize *IRAS* flux densities by integrating these extended spectra over the long *IRAS* system passbands. The corresponding ratios of synthetic 60 and 100 μm flux densities predicted by Engelke functions to those observed by *IRAS* (the FSS) are: 0.964 ± 0.013 (60 μm) and 0.976 ± 0.037 (100 μm). These should be compared with the corresponding numbers in the first line of Table 6. Differences are only at the 1.6σ level, so we could not discriminate statistically between Engelke approximations and true models of the infrared continuum solely on the basis of *IRAS* flux densities. The fundamental limitation again lies in the "RELUNCs."

10. CONCLUSIONS

We have assembled absolutely calibrated, complete, continuous stellar spectra for five cool stars: α Boo (updated), γ Dra, α Cet, γ Cru, and μ UMa. These spectra are constrained by carefully characterized photometry and have an estimated absolute uncertainty (within our adopted absolute framework: Paper I) of order 3% (1σ) across most of the 1.2–35 μm range. Such spectra establish the pedigree for secondary stellar standards and thereby the flexibility to calibrate arbitrary filter systems and sensors on the ground, from airplanes, or satellites. We find good agreement in shape between these spectra and generic Kurucz model atmosphere spectra, with the obvious exception of the SiO fundamental and some systematic small (~10%) deviations associated with the CO fundamental. Stellar angular diameters derived from our spectra are in accord with directly measured diameters.

Using a grid of computed stellar model continua, we have extrapolated our observed spectra as far as 300 μm, maintaining our absolute context, to provide calibration support for the *ISO* PHT and LWS instruments. Tests of these extrapolations using *IRAS* 60 and 100 μm point source flux densities show consistency with our predictions. The composite spectra with their associated pedigree files will appear on an AIP Journal CD-ROM and eventually will be obtainable through NASA's NSSDC at Goddard Space Flight Center.

REFERENCES

Alonso, A., Arribas, S., & Martinez-Roger, C. 1994, A&A, 282, 684

Barnes, T. G., Evans, D. S. & Moffett, T. J. 1978, MNRAS, 183, 285

Blackwell, D. E., & Lynas-Gray, A. E. 1994, A&A, 282, 899

Blackwell, D. E., Lynas-Gray, A. E., & Petford, A. D. 1991, A&A, 245, 567

Blackwell, D. E., Petford, A. D., Arribas, S., Haddock, D. J., & Selby, M. J. 1990, A&A, 232, 396

Brown, J. A., Johnson, H. R., Alexander, D. R., Cutright, L. C., & Sharp, C. M. 1989, ApJS, 71, 623

Carbon, D. F., & Gingerich, I. 1969, in Theory and Observations of Normal Stellar Atmospheres, edited by O. Gingerich (MIT Press), p. 377

Carbon, D. F., Langer, G. E., Butler, D., Kraft, R. P., Trefzger, Ch. F., Suntzeff, N. B., Kemper, E., & Romanishin, W. 1982, ApJS, 49, 207

Carter, B., 1996 (an Appendix in Paper VIII)

Cohen, M., & Davies, J. K. 1995, MNRAS 276, 715 (Paper V)

Cohen, M., Walker, R. G., Barlow, M. J., & Deacon, J. R. 1992a, AJ, 104, 1650 (Paper I)

Cohen, M., Walker, R. G., Carter, B., Hammersley, P. L., Kidger, M., & Noguchi, K. 1996b, in preparation (Paper VIII)

Cohen, M., Walker, R. G., & Witteborn, F. C. 1992, AJ, 104, 2030 (Paper II)

Cohen, M., Witteborn, F. C., Bregman, J., Wooden, D., Salama, A., & Metcalfe, L. 1996a, AJ, 112, 241 (Paper VI)

Cohen, M., Witteborn, F. C., Carbon, D. F., Augason, G. C., Wooden, D., Bregman, J., & Goorvitch, D. 1992b, AJ, 104, 2045 (Paper III)

Cohen, M., Witteborn, F. C., Walker, R. G., Bregman, J., & Wooden, D. 1995, AJ, 110, 275 (Paper IV)

Deacon, J. R. 1991, Ph.D. distertation, University College London

Di Benedetto, G. P. 1993, A&A, 270, 315

Di Benedetto, G. P., & Rabbia, Y. 1987, A&A, 188, 114

Engelke, C. W. 1992, AJ, 104, 1248

Gezari, D. Y., Schmitz, M., Pilts, P.S., & Mead, O. M. 1993, "Catalog of Infrared Observations," 3rd. ed., NASA RP-1294.

Glaccum, W. 1990, Ph.D. dissertation, University of Chicago

Gustafsson, B., Bell, R. A., Eriksson, K., & Nordlund, A. 1975, A&A, 42, 407

Hammersley, P. L. 1995 (an Appendix in Paper VIII)

Hoffleit, D., & Warren, Jr., W. H. 1991, Yale Bright Star Catalog, 5th revised ed. (NSSDC)

IRAS Explanatory Supplement 1988, "*IRAS* Catalogs and Atlases. Volume 1," NASA RP-1190 (GPO, Washington, DC)

IRAS Point Source Catalog, version 2, 1988, "*IRAS* Catalogs and Atlases. Volumes 2–6," NASA RP-1190 (GPO, Washington, DC) (PSC)

de Jager, C., & Nieuwehuizen, H. 1987, A&A, 177, 217

Judge, P. G., & Stencel, R. S. 1991, ApJ, 371, 357

Kholopov, P. N., *et al.* 1992, General Catalogue of Variable Stars, 4th ed. .(Mauka Publishing House, Moscow)

Kirby-Docken, K., & Liu, B. 1978, ApJS, 36, 359

Kurucz, R. L. 1991, "New lines, new models, new colors," in Precision Photometry: Astrophysics of the Galaxy, edited by A. G. Davis Philip, A. R. Upgren, and K. A. Janes (L. Davis Press, Schenectady), p. 27

Kurucz, R. L. 1993, CD-ROM series; "ATLAS9 Stellar Atmosphere Programs and 2 km/s grid" (Kurucz CD-ROM No. 13); "SYNTHE Spectrum Synthesis Programs and Line Data" (Kurucz CD-ROM No. 18)

Lord, S. D. 1992, "A New Software Tool for Computing the Earth's Atmospheric Transmission of Near-Infrared and Far-Infrared Radiation," NASA TM-103957

Moseley, S. H., Dwek, E., Glaccum, W., Graham, J. R., Loewenstein, R. F., & Silverberg, R. F. 1989, ApJ, 347, 1119

Moshir, M., *et al.* 1992, Explanatory Supplement to the *IRAS* Faint Source Survey, Version 2, JPL D-10015 JPL, Pasadena

Mozurkewich, D., Johnston, K. J., Simon, R. S., Bowers, P. F., & Gaume, R. 1991, AJ, 101, 2207

Ridgway, S. T., Jacoby, G. H., Joyce, R. R., Siegel, M. J., & Wells, D. C. 1982, AJ, 87, 1044

Ruland, F., Biehl, D., Holweger, H., Griffin, R., & Griffin, R. 1980, 92, 70

Scholtz, M., & Takeda, Y. 1987, A&A, 186, 200

Selby, M. J., Hepburn, I., Blackwell, D. E., Booth, A. J., Haddock, D. J., Arribas, S., Leggett, S. K., & Mountain, C. M. 1988, A&AS, 74, 127

Sinton, W. M., & Tittemore, W. C. 1984, AJ, 89, 1366

Stencel, R. S. 1996 (private communication)

Strecker, D. W., Erickson, E. F., & Witteborn, F. C. 1979, ApJS, 41, 501

Sylvester, R. 1996 (private communication)

VandenBerg, D.A., & Laskarides, P. G. 1987, ApJS, 64, 13

van der Blieck, N. S., Gustafsson, B., & Eriksson, K. 1996, A&A (in press)

Witteborn, F. C., & Bregman, J. D. 1984, Proc. Soc. Photo-Opt. Instr. Eng., 509, 123

White, N. M., & Feierman, B. H. 1987, AJ, 94, 751

Witteborn, F. C., Cohen, M., Bregman, J. D., Heere, K. R., Greene, T. P., & Wooden, D. H. 1995, in Proceedings of the Airborne Astronomy Symposium on the Galactic Ecosystem, edited by M. Haas, E. F. Erickson, and J. Davidson (in press)

Wooden, D. H. 1989, in Proceedings of ESO SIPC Workshop, SN 1987A and Other Supernovae, edited by I. J. Danziger and K. Kjar (ESO, Garching), p. 531